Article submitted to: High Power Laser Science and Engineering, 2023 *June 19, 2023*

Spectral purity systems applied for Laser-produced plasma Extreme UltraViolet (LPP-EUV) lithography source: a review

Nan Lin[1,2,†,*], Yunyi Chen[1,2,†], Xin Wei[1,2], Wenhe Yang[1,2], and Yuxin Leng[2,*]

[1]*School of Microelectronics, Shanghai University, Shanghai 200072, China*
[2]*Department of Precision Optics Engineering, Shanghai Institute of Optics and Fine Mechanics, Chinese Academy of Sciences, Shanghai 201800, China*

Abstract
With the development of high volume manufacturing for very large scale integrated circuit, the purity of the light source in the extreme ultraviolet lithography (EUVL) system needs to fulfill extreme requirments in order to avoid thermal effect, optical distortion and critical dimension errors caused by out-of-band radiations. This paper reviews the key technologies and developments of the spectral purity systems for both free-standing system and build-in system integrated with the collector. The main challenges and developing trends are also discussed, with a view towards practical applications for further improvement. Designing and manufacturing spectral purity systems for EUVL is not a single task, it requires systematic considerations for all relevant modules. Moreover, the requirements of spectral purity filters drives the innovation in filtering technologies, optical micromachining and advanced metrology.

Keywords: Spectral purity filter; Extreme UltraViolet Lithography; Collector mirror

1. Introduction

As the main technical support for the development of the semiconductor industry, lithography can be considered as the foundation of the current global information industry. In 1965, Gordon Moore followed the development trend of integrated circuits at the time, and proposed that the number of transistors on the integrated circuit would double every about 18 months, which was the "Moore's Law"[1] that the industry has been catching up with till now. The revolution of microchip integration puts forward higher demands on the lithography technology. According to the Rayleigh criterion[2], Equation (1), the resolution of the lithography process can be improved by reducing the wavelength of the exposure light source or increasing the numerical aperture (NA) of projection lens.

$$Resolution = k_1 \frac{\lambda}{NA} \tag{1}$$

where λ is the wavelength of the exposure light source, k_1 is the process constant. Currently, the lithography machine with the shortest working wavelength uses the 13.5nm (2% bandwidth) extreme ultraviolet (EUV) light. Generally, there are four ways to produce 13.5nm EUV radiation: synchrotron radiation source, discharge produced plasma (DPP), laser-assisted discharge plasma (LDP), and laser produced plasma (LPP). Among them, the synchrotron radiation source[3] can produce high power EUV radiation with no debris, but the device structure is complex and expensive; DPP[4] and LDP[5] methods will lead to heat load and corrosion on the electrode, resulting in damage of key components; relatively, the light source generated by LPP[6] is much more stable, and the amount of debris is less than with DPP, making it the mainstream of EUV lithography (EUVL) light source.

The LPP-EUVL light source system mainly consists of three parts which are the driven laser, Sn droplet targets and the collector, as shown in Figure 1. The light source system is designed in the shape of an ellipse-of-revolution[8], with one foci where Sn droplets are hit and the other far away from the collector called the intermediate focus (IF). The pre-pulse laser (e.g., 1064nm Nd: YAG laser) firstly gasifies and partially ionizes the droplet target, and then the main-pulse laser (e.g., 10.6um CO_2 laser) completely ionizes the steam group to produce a stronger EUV radiation.[9] After

† These authors contributed equally to this work.
Correspondence to: Nan Lin and Yuxin Leng. Department of Precision Optics Engineering, Shanghai Institute of Optics and Fine Mechanics, Chinese Academy of Sciences, Shanghai 201800, China. Email: nanlin@siom.ac.cn (N. Lin); lengyuxin@mail.siom.ac.cn (Y. X. Leng)

10.1017/hpl.2023.53
https://doi.org/10.1017/hpl.2023.53 Published online by Cambridge University Press

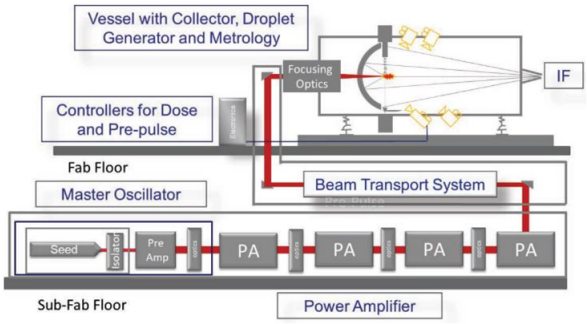

Figure 1. Schematic of LPP-EUVL source system. Figure from Ref. [7]

that, the collector concentrates and reflects the radiations to the IF for the subsequent optical path propagation.[10]

As one of the most important sub-modules, the collector is a multilayer-coated mirror which is in the shape of the graded ellipsoid with 5.5sr.[7,11,12] With it, the EUV generated can be collected and concentrated to the IF, as shown in Figure 2. In order to satisfy actual production requirements of the EUV with high efficiency, high power and high purity, the collector needs to meet some design specifications[8], such as: a large enough solid collecting angle of 5.5sr[7,11,12], highly reflective multilayer coating, as well as some specific designs to reduce the thermal load of the collector, such as the water-cooling device. However, the collector meeting the above requirements at the same time can also transmit the out of band (OoB) radiations, i.e., the radiations other than 13.5nm (2% band) EUV. Once the OoB radiations are introduced or generated, the light collected and reflected by the collector will no longer be pure, which will not only influence the lithography performance, but also reduce the lifetime of the collector. Thus, it is necessary to design a spectral purity filter (SPF) in the EUVL system to filter out these OoB radiations.

In the past few years, different types of SPFs for EUVL have been designed and manufactured, and some have shown good performance. However, there are no comprehensive reviews and analyses of the research in this field to reflect the latest progress and the existing problems for further study. This paper reviews and discusses the technologies of filtering out OoB radiations in the LPP-EUVL system. Firstly, the influences of OoB radiations on the lithography performance are given. Then, the principles and recent progress of SPFs for EUVL are reviewed, which is introduced from the aspect of free-standing systems and the built-in systems. Major challenges needed to be solved, including the OoB suppression, manufacturing process as well as different metrologies, etc., are discussed. The technical routes of ASML and Gigaphoton Inc. are specifically discussed. Finally, the future development of SPFs for EUVL is expected in the view of practical applications.

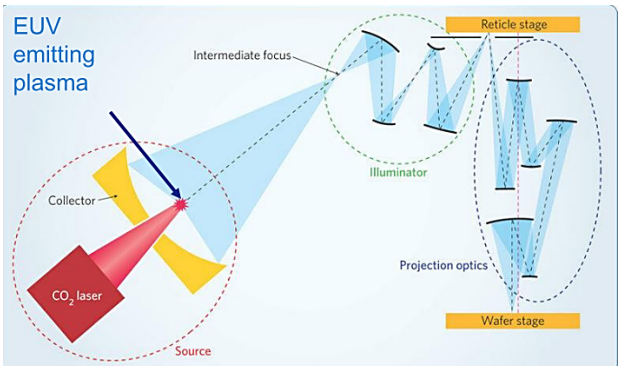

Figure 2. Role of the collector in the light source system: Collector collects radiations and reflect them to the IF for subsequent optical path propagation. Figure from Ref. [13]

2. OoB radiations of the EUVL light source

In the light source system, the driven laser hits each Sn droplet target twice to completely ionize it and generate EUV radiation. However, this process not only generates EUV radiation, but also introduces OoB radiations, which are listed in Table 1.

Table 1. Radiations in EUVL light source [14]

Radiation	Wavelength (nm)
(In-band) EUV	13.5 ±2 %
EUV-OoB	5-70 excluding (in-band)EUV
VUV	70-130
DUV	130-400
VIS	400-800
IR	> 800

At present, the collector is generally deposited with Mo/Si multilayers to achieve high EUV reflectivity.[11] Figure 3 shows the reflectivity of Mo/Si multilayers to different radiations. It can be found that the EUV reflectivity is close to 70%, while the EUV-OoB reflectivity is so low that it can be neglected. The reflectivity of ultraviolet (UV)/visible spectrum (VIS) is relevant to EUV, and the reflectivity of infrared radiation (IR) is nearly 100%. If all these OoB radiations are reflected by the collector and propagate to the subsequent optical path, the performance of the system will be greatly reduced.

For the vacuum ultraviolet (VUV) radiations, they are effectively removed by the background hydrogen, which is originally designed for the debris mitigation.[16] The deep ultraviolet (DUV) radiation above 300nm (i.e., 300-400nm) and VIS have little impact on the lithography performance because the specifically designed photoresist is generally insensitive to it.[17] In fact, the radiations which have a significant influence on lithography are IR and DUV (130-300nm). Therefore, most filters in the EUVL system are mainly designed for these two wavelength ranges.

https://doi.org/10.1017/hpl.2023.53 Published online by Cambridge University Press

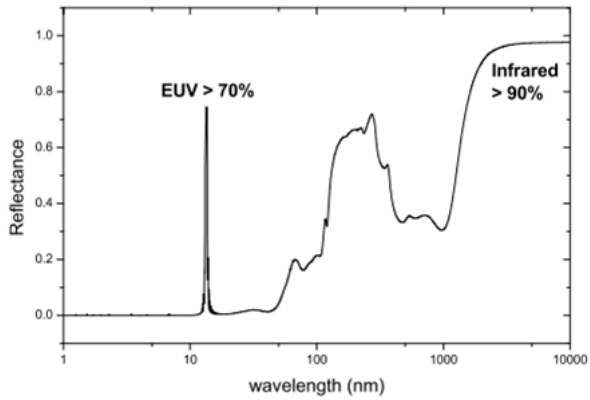

Figure 3. Calculated reflectance of the 50-bilayer Mo/Si multilayer coating of 6.9nm periodicity. Figure from Ref. [15]

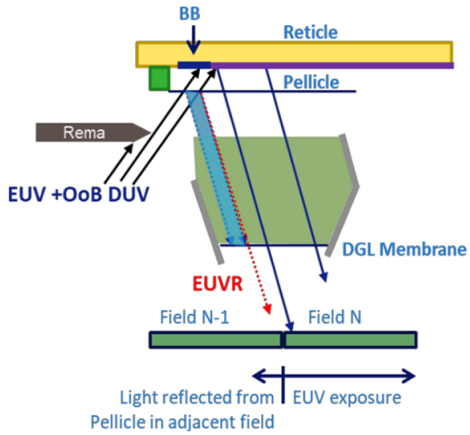

Figure 4. Black border's influence on CD errors of the corners and edges of the adjacent field. Figure from Ref. [25]

2.1. Infrared radiation

IR comes from the driven lasers (i.e.,10.6um CO_2 lasers and 1064nm Nd: YAG laser) of the LPP-EUVL light source.[18] When generating EUV, the redundant IR of the lasers will also be reflected by the collector and propagated by all the following mirrors, as shown in Figure 2. In the case of the main-pulse CO_2 laser with the power of $\sim$20kW, there's $\sim$10% of the power (i.e., $\sim$2kw) that can be collected at the IF.[19] Such high power radiation will lead to the heating phenomenon[15,18,20] of optics, reticles, and wafers, which may cause severe optical distortion and reduce pattern accuracy. For example, since the redundant IR at IF can be 3-5 times that of the EUV radiation, the overlay error may exceed 8 times the specification.[21] The other problem is that the mirror heating may lead to mutual diffusion of multilayers, photon-assisted oxidation[22], etc., and these will reduce the lifetime of optics and even destroy them.

Therefore, the intensity of IR is required to be less than 10% of the EUV at the wafer to relieve the damage, which means it needs to be 0.2% or even less of the EUV at the IF.[10,12]

2.2. Deep ultraviolet

The Sn droplet target hit by the laser will ionize and produce Sn plasma. EUV are generated by the ion transition of $Sn^{7+}\sim Sn^{10+}$, whereas DUV are mainly generated by Sn^{1+},Sn^{2+} and Sn^{3+}.[16] The resist is very sensitive to the DUV from 150 to 300nm[17,23] which may lead to unwanted background exposure of resist, resulting in the loss of image contrast and critical dimension (CD) bias.[16,17] As depicted in Figure 4, in the exposure system, the DUV reflection at the black border (BB) on a reticle will overexpose the corners and edges of the adjacent field. What's more, in order to prevent the reticle from being polluted, a pellicle is placed on the surface of it. ASML has already invented the pellicle with 90.6% EUV transmissivity.[24] This kind of pellicle has a higher reflectivity of DUV than BB, so it will have a greater impact on the CD at the corners and edges.[14] However, in practice, the wavelengths below 250nm are usually suppressed due to the reflection of mirrors in the illumination and projection systems[16], so DUV plays a limited role.

In contrast to IR, the intensity of DUV is related to the characteristics of the droplet, laser effects and even some unknown elements, such as the optical column reflectivity of DUV, the DUV emission angular dependency of the plasma, etc.[16] Thus, the DUV performance is generally evaluated with the dose-to-clear exposure measurement at the wafer level rather than the IF point, as the Equation (2) represents.[16,23] The ratio of DUV and EUV is determined by the dose-to-clear from both multilayers and chromium of the reticle. To meet the qualification of the EUVL, the value is limited to less than 1% at the wafer.[10,12]

$$\frac{DUV}{EUV} = \frac{E_0^{ML}}{E_0^{Cr}} \cdot 100\% \tag{2}$$

3. Free-standing SPFs

Since IR and DUV greatly degrade the performance of lithography, it is necessary to filter them out to keep high spectral purity. In the past few years, different kinds of spectral purity filters (SPF) have been designed and applied into the EUVL system. They can be generally divided into two kinds: free-standing systems and built-in systems. The former refers to the filters that serve as independent devices in the source system, including the transmissive SPF and reflective SPF. The latter refers to the structures that are integrated with the collector, which will be discussed in Section 4.

3.1. Transmissive SPF

A transmissive SPF, which has the structure of periodic multilayers of high and low refractive index materials, is

https://doi.org/10.1017/hpl.2023.53 Published online by Cambridge University Press

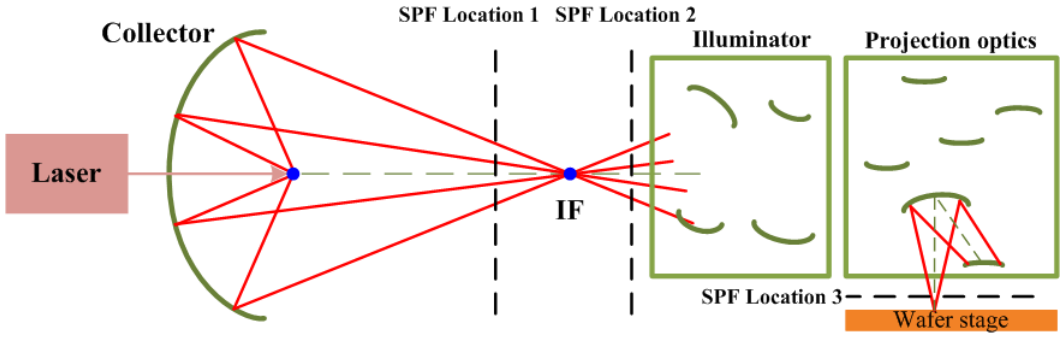

Figure 5. EUVL system with possible locations for the transmissive SPF.

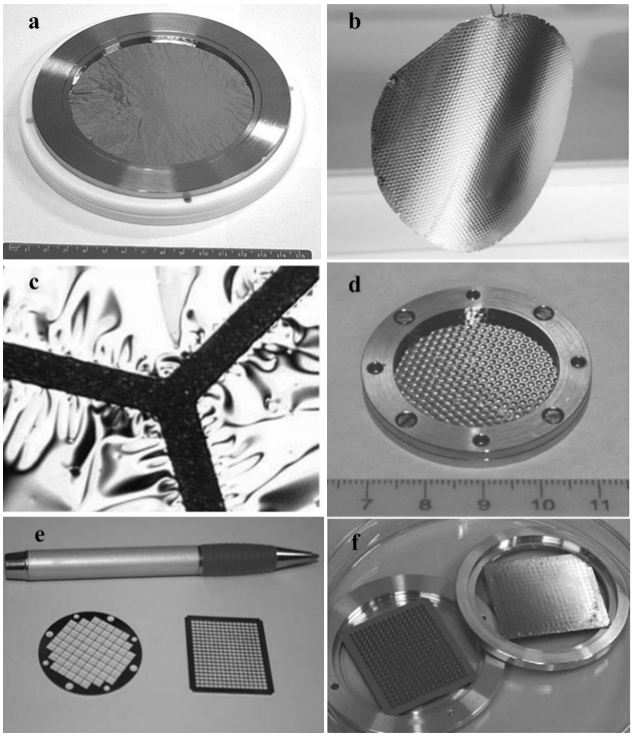

Figure 6. Foil transmissive SPFs with different designs to improve mechanical strength: (a) Zr/Si foil SPF surrounded with a rigid frame, (b) a leaf of mesh supported Zr/Si film, (c) a detailed mesh structure of (b), (d) Zr/Si SPF with (b) film and a rigid frame, (e) Samples of steel mesh, (f) Glued Zr/Si SPFs of (e) structure. Figure from Ref. [26]

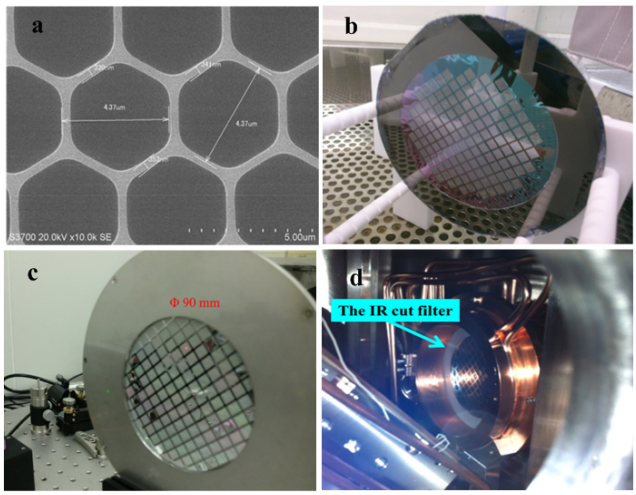

Figure 7. Grid transmissive SPF of IR suppressing: (a) SEM image of the grid after etching, (b) Grid SPF after backside wet etching, (c) Grid SPF with a diameter of 90 mm installed for measurement, (d) Grid SPF installed in LPP source system. Figure from Ref. [19]

designed to reflect or absorb OoB radiations but transmit EUV radiations. Typical transmissive SPFs include foil filters[26], grid filters[19,21], etc. The transmissive SPF is usually placed before or after the IF, but in some special cases, it is placed between the projection optics and the wafer, as depicted in Figure 5. The transmissive SPF for commercial EUVL needs to meet three primary requirements, including maintaining high transparency at 13.5 nm (2%), effectively suppressing out-of-band (OoB) radiation, and possessing sufficient mechanical strength.

To achieve high EUV transmissivity, a transmissive SPF needs to remain high transparency at 13.5nm (2%) over a long working time. In contrast to monolayer films, intermetallic membranes have a better performance in IR suppression[27], thus multilayers composed of different high-transparency materials are studied. Andreev et al.[28] has compared the performance of filters for EUV, which are constructed with Zr/Si, Nb/Si, Mo/Si or Mo/C multilayers. Bibishkin et al.[26] fabricated a Zr/Si filter with a transparency of 76%, and achieved an EUV transmittivity of 78% and suppression ratios from 1000 (UV) to 25 (near IR). Chkhalo et al.[27] later found that adding a metallic coating layer and using silicide instead of silicon can relieve the oxidation effect in multilayers. Therefore, they fabricated a $Zr/ZrSi_2$ filter coated with $MoSi_2$ and its transparency only decreased by 4.8%, while the uncoated one decreased by about 10%. Subsequently, they substituted Zr layers with Mo layers and achieved a better performance with an in-band transparency above 70%[29]. Notably, choosing proper materials is a trade-off among EUV transparency, OoB suppression and mechanical strength. Although some

https://doi.org/10.1017/hpl.2023.53 Published online by Cambridge University Press

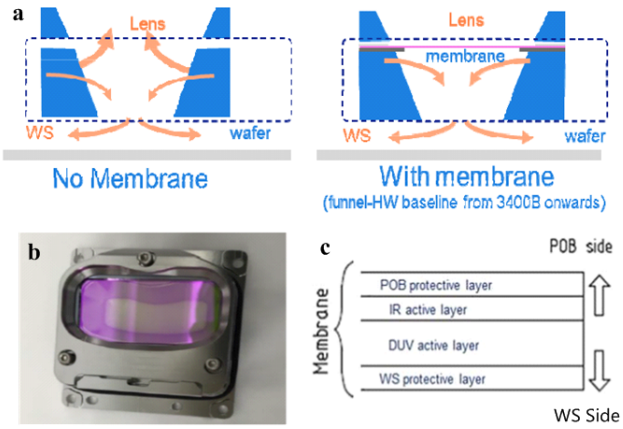

Figure 8. Details of DGLm: (a) DGL's location and its influence on outgassing suppression, (b) a figure of DGLm sample, (c) schematic of DGLm stack build-up. Figure from Ref. [30, 31]

materials perform well in transparency, their mechanical strength is not ideal for high power laser, such as Mo/$MoSi_2$ multilayers[27].

To withstand a long-time heat load, a filter needs to have enough mechanical strength to ensure that it won't be broken by radiations. Bibishkina et al.[26] manufactured filters with different structures to improve the mechanical strength, such as the simple filter with a rigid framework, the improved structure with a mesh structure or a rigid mesh structure, as shown in Figure 6. However, these filters still cannot meet the requirements of commercial EUVL. To go further, Soer et al.[21] developed a honeycomb grid SPF with an EUV transmittance of 72% at normal incidence, which can stand a CO_2 laser power density of 100 W/cm2 for 8 hours. Suzuki et al.[19] also adopted the honeycomb grid structure to produce an IR cut-off filter with a diameter of 90 mm for EUV light source, as shown in Figure 7, and finally achieved 99.7% suppression for 10.6um, but the transmittance of EUV is about 78%, which still leads to considerable EUV loss.

3.1.1. ASML's technical route In the EUVL system of ASML, the reticle is protected from being contaminated by covering a pellicle on it which has a higher reflectivity to DUV than BB, resulting in a greater impact on CD errors. To reduce its influence, a free-standing transmissive SPF, which is called dynamic gas lock membrane (DGLm), is adopted by ASML in NXE:3400. Figure 8 depicts the details of the DGLm. The DGLm is mainly composed of four different layers[30], of which DUV and IR active layers are the core of the whole membrane to filter out the OoB radiations. Different to most transmissive SPFs' location, the DGL membrane is located between the projection optics and the wafer. With this design, the DGL membrane acts as a physical barrier to prevent the contamination of projection optics caused by resist outgassing.[32] The DGL membrane is a free-standing device, thus it can be replaced once damaged.

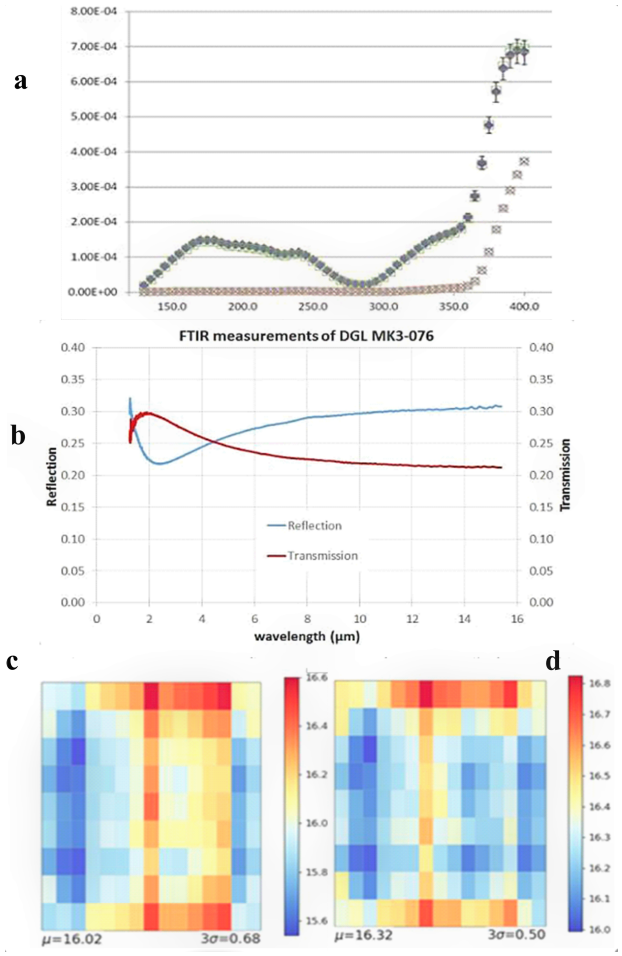

Figure 9. OoB suppression performance with DGLm: (a) complete suppression of DUV (<0.1% transmitted) as measured by PTB, (b) 78% IR suppression as measured off-line by FTIR; Intra-die fingerprint of 16nm Dense Lines/Spaces showing (c) edge/corner effect without DGLm, (d) edge/corner effect with DGLm. Figure from Ref. [16, 30]

What's more, as the membrane is placed further away from the IF, it is less sensitive to non-uniform transmission and particles[30].

With the design of DGLm, more than 99% DUV and nearly 80% IR can be suppressed[30], as depicted in Figure 9. Since the total thickness of the membrane is below 50nm and the absorption coefficient of the material is low, the EUV transmittance can reach 85%.[30] Without the DGLm, the CD at corners and edges are all less than 0.1nm, which has already met the requirements of N5 node, while with the DGLm, CD reaches ~0.04nm[16], which represents an improvement of DUV suppression. It should be noted that the excellent performance without DGLm is based on the suitable solutions of other EUVL components, such as the specific designs of the black border and the sensitive enough resist, but DGLm can improve the DUV suppression under conditions not that good enough, such as the less sensitive resist, etc. However, a potential problem is that the OoB light is not filtered until it enters the wafer stage, the mirrors in the

https://doi.org/10.1017/hpl.2023.53 Published online by Cambridge University Press

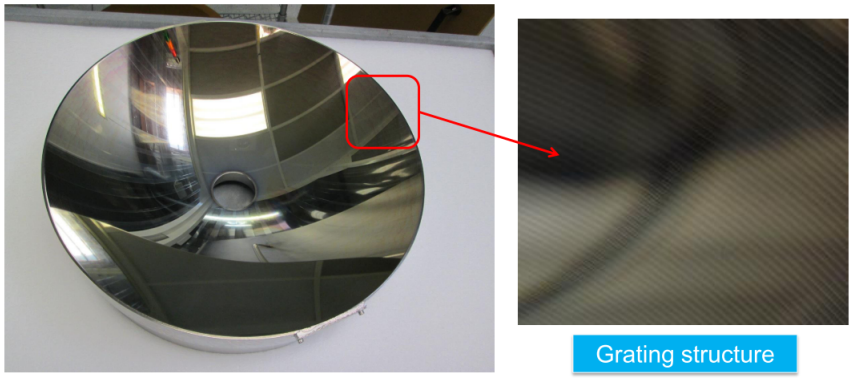

Figure 10. Collector with a grating structure from Gigaphoton. Figure from Ref. [34]

optical path will be damaged by the high-power radiation.

3.2. Reflective SPF

The reflective SPF is designed to reflect EUV, but diffract or absorb the OoB. It is usually a composite grating structure with multilayers deposited on the surface. A typical study by Kierey et al.[33] manufactured a blazed grating SPF, which is composed of grating segments with different linear densities.The blazed grating is made of NG5 black glass and coated with the Ru layer. Its blazed angle is optimized to $1.2° \pm 0.2°$. One of the segments was measured on BESSY II, and showed that the EUV reflectivity reached 57% at the incident angle of $83°$. The structure of the free-standing reflective SPF allows it to be designed onto the EUV collector, so the relevant researches on it are mainly focused on the early stage, which also provided a certain theoretical basis for the collector integrated with a grating structure. They will be discussed in combination with build-in SPFs in Section 4.

Comparing the above two SPFs, it can be found that the reflective SPF has better robustness and can be designed onto the collector to reduce one optical element, although the EUV reflectivity may be limited to the collector efficiency (i.e., 70%). The advantage of the transmissive SPF is that it doesn't change the optical path of EUV, so the design of the optic system has little or even no impact. Nevertheless, both two SPFs are free-standing devices which are easy to be broken by the OoB, especially IR. Therefore, the build-in spectral purity filtering systems have been proposed and become one of the mainstream schemes.

4. Integrated SPFs on the collector

The built-in SPF system refers to the collector integrated with grating structures, as shown in Figure 10. This design not only reduces an optical element in the light source system, but also has a better mechanical strength, and the water-cooled device fabricated on the collector in some designs also reduces the thermal effect. There are mainly two technical routes of fabricating gratings on collectors[35], one is to etch / deposit gratings on multilayers which is introduced in section 4.2, the other is to fabricate gratings directly on the collector substrate and then followed by coating which is introduced in section 4.3. The latter method is one of the mainstream methods, and has already been maturely applied to the EUVL light source system[8,36,37].

4.1. Principles

The principles of the collector integrated with gratings are based on the Bragg reflection by the multilayers and the diffraction due to the predetermined grating shapes[38].

4.1.1. Bragg diffraction The EUV collector is also known as a Bragg reflector[39] for the design of coating Mo/Si multilayers on the surface of the collector to maximize the EUV reflectivity. The Bragg reflector is an optical device that uses the constructive interference of reflected light at different interfaces to enhance the reflection of specific wavelengths.[40,41] According to the Bragg's Law, when the optical path difference of the reflected light at two adjacent interfaces is half a wavelength, the reflected light at the interface will occur constructive interference and get a strong reflection[42]. Equation (3) gives the formula formation of the Bragg's Law in the case of periodic multilayers[43,44].

$$2dsin\theta = n\lambda \tag{3}$$

where d is the multilayer period, θ is the incident angle, n is diffraction order, λ is the incident wavelength. The reflectivity is determined by the number of layers and the refractive index difference between materials.

4.1.2. Grating diffraction Grating diffraction is generally based on the Fraunhofer multi-slit diffraction effect. Once the optical path difference from the two adjacent slits to the interference point is an integral multiple of the wavelength of the incident light, the two beams have the same phase, and

https://doi.org/10.1017/hpl.2023.53 Published online by Cambridge University Press

the interference will be enhanced[40]. Grating Equation (4) summarizes the phenomenon.

$$p(sin\delta + sin\theta) = m\lambda \tag{4}$$

where p is the grating period, δ is the diffraction angle, θ is the incident angle, m is the diffraction order, and λ is the wavelength of the incident light. With proper grating designs according to Grating Equation, the needed radiation can be concentrated around one specific diffraction order, and most of the OoB radiation is diffracted to other orders[36,45,46].

Figure 11 shows the schematic of the OoB suppression design with the build-in SPF system, in which the blue line is the beam path of EUV, while the red line is OoB. After the laser radiations hitting the Sn droplets, the EUV generated and the OoB radiations travel to the collector firstly. With the effect of the grating coated with Mo/Si multilayers, the EUV concentrated at the zero order is reflected to the IF for the subsequent propagation, while the IR is diffracted to higher diffraction orders and stopped by the beam stop.

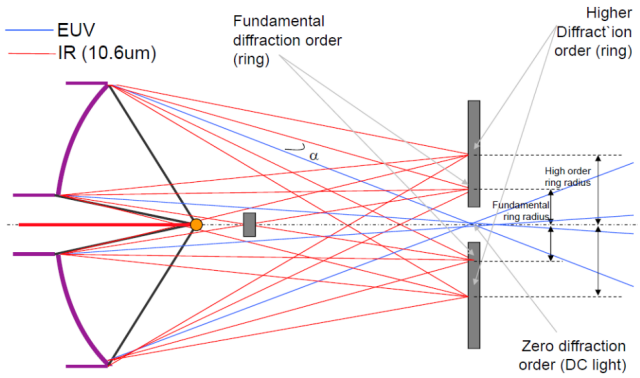

Figure 11. Schematic of the IR suppression design with the collector integrated with the rectangular substrate grating. Figure from Ref. [65]

4.2. *Multilayer gratings*

The multilayer grating refers to etching / depositing multilayers in the shape of gratings on the substrate of the collector.[47,48] Spiller[49,50] firstly suggested to use the reflective multilayers to improve the EUV reflectivity of the grating.[51] Figure 12 depicts the schematic of the rectangular multilayer grating. The rectangular grating is not only easy to fabricate, but also effective to suppress the specific wavelength, thus it is often considered as a good solution to the build-in SPF system. Boogaard et al.[39] generated a Mo/Si rectangular multilayer grating reflector for EUVL which provided a 64% EUV reflectivity with a 30 times suppresion at 280nm. Trost et al.[48] designed a Mo/Si multilayer grating which generated only 0.04% IR with an EUV reflectivity of 53% at zero order. Medvedev et al.[45] adopted the lift-off contact lithography process to fabricate the multilayer grating and achieved 61% EUV reflectivity

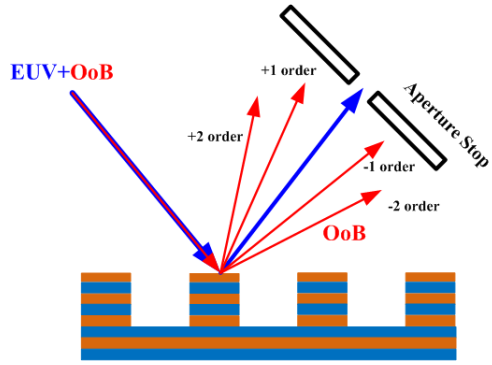

Figure 12. Schematic of the rectangular multilayer grating.

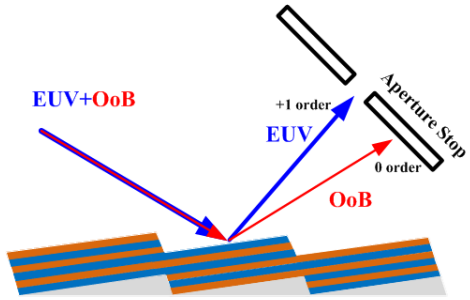

Figure 13. Schematic of the blazed multilayer grating.

with 70 times suppression at 10um. The process allowed a much shorter grating period to meet a better angular separation for EUV and OoB. However, the rectangular multilayer grating can only be used to suppress a single wavelength, and is difficult to achieve high EUV diffraction efficiency (DE) while eliminating OoB.

Compared with the rectangular grating, the blazed grating can suppress a wider range of wavebands[52], as shown in Figure 13. Naulleau et al.[53] analysed the main factors that affect the EUV and OoB efficiency in the EUVL light source system, and proposed a theoretical efficiency analysis of the blazed grating SPF. Boogaard et al.[15] demonstrated theoretically that the full spectral separation can be obtained without losing EUV reflectance if the multilayer performance is not influenced by the process. Generally, the DE of the multilayer blazed grating is effected by the quality of saw-tooth facets, smoothness of the substrate, and groove density, and the former two are the main challenges. Naulleau et al.[51,54,55] proposed a method of fabricating the blazed grating and decreased the roughness caused by the substrate by using the smoothing optimized multilayers which presented an evident smoothing effect, while it was at the cost of the profile fidelity. Liddle et al.[54,56] identified the conditions for topography control while fabricating the blazed grating with hydrogen silsesquioxane (HSQ), and achieved a relative EUV efficiency of 63%. Voronov et al.[57] optimized the growth of Mo/Si multilayers by varying the sputtering gas pressure, and improved the DE from 39.6% to

https://doi.org/10.1017/hpl.2023.53 Published online by Cambridge University Press

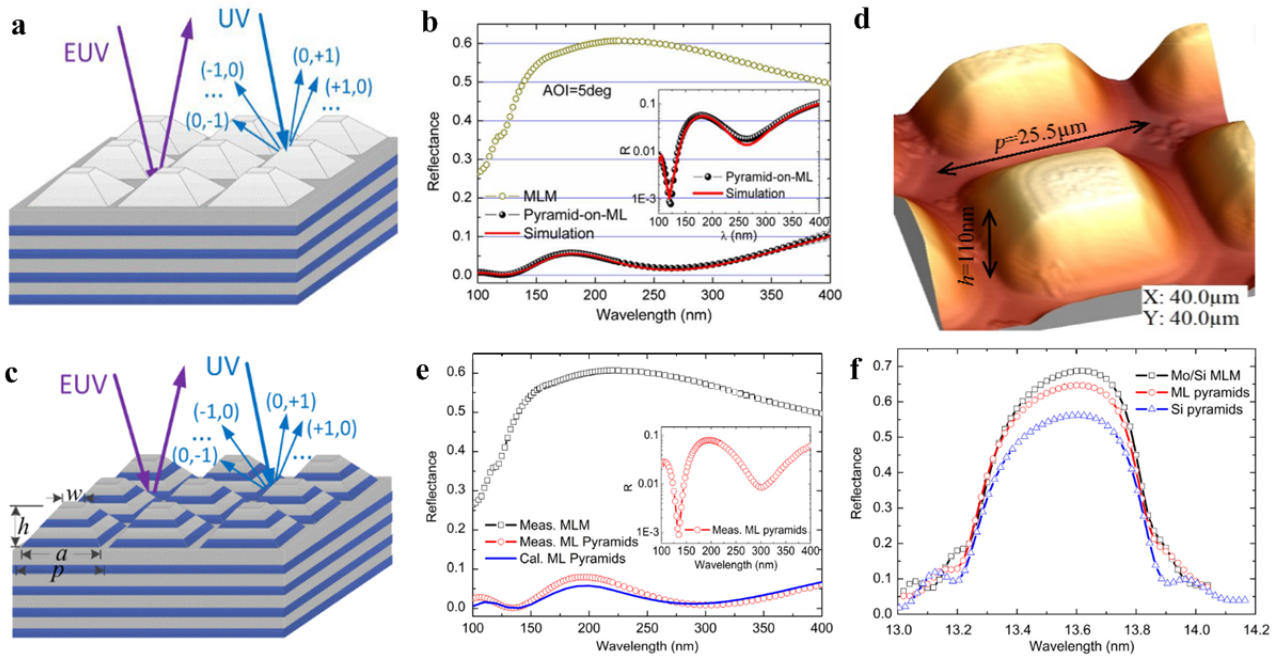

Figure 14. 2D pyramid multilayer grating on the collector: (a) Si pyramid on Mo/Si multilayers, (b) UV-suppression performance of (a) and the unstructured multilayers, (c) Mo/Si pyramid on Mo/Si multilayers, (d) AFM image of (c), (e) UV-suppression performance of (c) and the unstructured multilayer, (f) EUV performance comparison of (a) (c) and unstructured multilayers. Figure from Ref. [59, 60]

44.0%. The same group[58] then founded that the reduction of the groove density and the high-order operation can lead to higher efficiency. A 52% EUV DE was obtained at the second order with a 2525 lines/mm blazed grating. Miles[46] expounded the methodology of manufacturing the blazed grating and raised a way to replicate the grating which obtained 65% DE at first order. However, though numerous methods are raised to improve the process, it's still too difficult to meet the requirements, thus the DE of the blazed grating is far from the theoretical limit.

A new pyramid structure with a feasible process method, such as the half-shadowing, has been proposed to suppress the full DUV band, as shown in Figure 14. Initially, a 2D pyramid structure made of Si which was deposited on Mo/Si multilayers was preferred. Huang et al.[59] studied the mechanism of pyramid structure suppressing DUV, and the Si pyramid showed 0.1% - 10.5% DUV reflectivity which was about 14 times suppression compared with the non-structured collector, and the EUV's peak reflectivity reached 56.2%. To reduce the loss of EUV, the Mo/Si multilayer pyramid was proposed to replace Si pyramid and the EUV reflectivity was up to 64.7%, while the DUV response was the same as that of the Si pyramid.[47,60] Although the multilayer pyramid grating shows good performance within DUV filtering and EUV reflectivity, this structure has not been made and tested on the EUVL collector to the author's knowledge, and the performance in IR filtering also hasn't been studied.

The multilayer grating provides a method to integrate the grating structure with the collector, and has been widely studied in recent years. The key point, as well as the difficulty, of this technology is to develop a suitable process for stacking multilayers without degrading the EUV reflectivity[61]. In particular, the rectangular grating on the collector requires about 500 pairs of layers[48,61] with smooth surfaces and steep edges, etc., and this largely reduces the feasibility of using multilayer gratings as the SPF.

4.3. Substrate gratings

The substrate grating refers to the case that the surface of the collector substrate is firstly fabricated in the shape of the grating, and then the multilayers are deposited[35,61]. The method has advantages. It reduces an optical element in the light source system, has a good mechanical strength, and avoids the process difficulty of stacking hundreds of layers. This scheme has already been applied to the collector by Gigaphoton[37,62–64]. They adopted the rectangular grating as the substrate grating to filter out the IR of 10.6um and 1064nm, and achieved only 0.37% IR reflectivity[65,66], while the EUV reflectivity only reduced by ~4% compared with the mirror without grating structure[37].

This section will mainly discuss the rectangular substrate grating, including the design principles, fabrication process, and the metrology. Gratings of other shapes will also be introduced briefly as a supplement in 4.3.4.

https://doi.org/10.1017/hpl.2023.53 Published online by Cambridge University Press

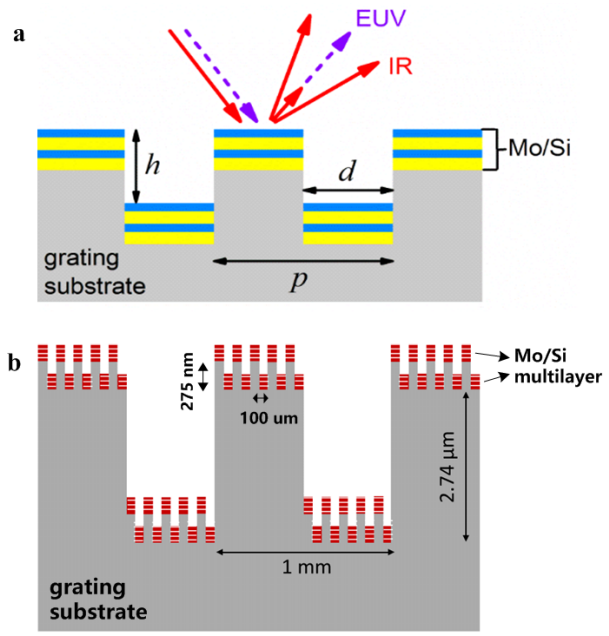

Figure 15. Design of the rectangular substrate grating: (a) Schematic of 1D rectangular substrate grating, (b) Schematic of 2D rectangular substrate grating by IOF. Figure from Ref. [45, 68]

4.3.1. Design principles Assuming that the OoB needed to be suppressed is 10.6um and the grating is in the shape of 1D rectangular. As Figure 15 shows, the grating is characterized by the period p, width d and depth h of the grooves. When the 13.5nm EUV combined with 10.6um incident onto the grating, if the diffraction order $m = 0$, both radiations' reflection angles are the same, while with higher diffraction orders, the characteristic values of the diffraction angles differ by about three orders of magnitude[45]. Therefore, the 10.6um radiation at m=0 is what we need to suppress. Assuming that the grating is illuminated by the normal-incidence plane wave, Equation (5) shows the m^{th} order DE of the 1D rectangular phase grating, and Equation (6) is the particular case of zero diffraction order which both can be derived from the Equation (2)[45].

$$R_n = R_{tot} \left| sinc(m\pi) + A\Gamma sinc(m\pi) \right|^2 \qquad (5)$$

where R_{tot} is the total reflected intensity, $\Gamma = \frac{d}{p}$ and $A = exp(\frac{i \cdot 4\pi h}{\lambda}) - 1$

$$R_0 = R_{tot}\{1 + 2\Gamma(\Gamma - 1)[1 - cos(\frac{4\pi h}{\lambda})]\} \qquad (6)$$

To suppress the 10.6um IR at zero order, the Equation (5) should equal to zero. It can be calculated that the fill factor $\Gamma = 0.5$ and the minimum depth of the grooves is $h = \frac{\lambda}{4} = \sim 2.65um$. The period p is more difficult to determine because it's a trade-off between IR reflectivity at zero order ($\sim p/\lambda$) and the angular separation of diffraction ($\sim arcsin(\lambda/p)$).[45,67] What's more, the limited spatial and temporal coherence of the radiation should also be considered.[45,60]

To suppress radiations of two wavelength, in particular 10.6um and 1064nm, this method can be used to determine the dual-layer grating. Since the difference between the two wavelengths is 10 times, the parameters of the grating are also 10 times different. The Fraunhofer Institute for Applied Optics and Precision Engineering (IOF)[36,61] designed and fabricated a dual-wavelength rectangular grating with optimized geometric paramters, as shown in Figure 15. At the IF, the measured reflectivity of 10.6um is 0.32%, the reflectivity of 1064nm is only 0.08%, and the average reflectivity of EUV at 13.5nm is 64% which represents only 4.5% loss compared to the unstructured multilayers.

4.3.2. Fabrication process At present, there are two main processes to fabricate the substrate gratings deposited with multilayers. The main difference of them is the preparation of the substrate grating, which are the diamond turning process and the ion beam etching.

The process of manufacturing the substrate grating used by Rigaku is the diamond turning[34]. Firstly, Ni is injected into the substrate made of Al alloy and the surface of it is polished. Then the grating grooves are made on the Ni surface by diamond turning, which will result in turning patterns, as shown in Figure 16 (a), and the high spatial frequency roughness (HSFR) on the cut surface. Therefore, a glass smoothing layer is then needed to smooth the substrate grating. The other method, ion beam etching process, is used by IOF[36,61] to prepare a dual-layer rectangular grating on the collector's substrate which is made of AlSi alloy. With the method, the substrate is firstly diamond turned and polished to reduce the HSFR to less than 0.2nm rms, and then, the dual-layer grating is directly constructed into the NiP layer of AlSi substrate by ion beam etching.

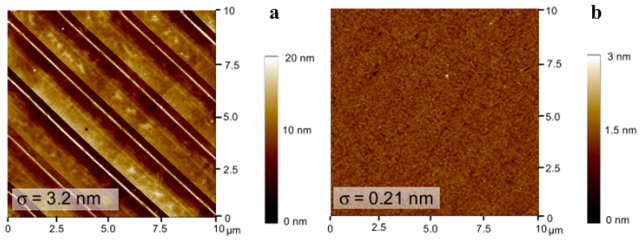

Figure 16. (a) AFM image of diamond turned patterns, (b) Mechanical polished surface of (a). Figure from Ref. [48]

When manufacturing the substrate grating, HSFR is a critical factor to achieve a smooth enough surface. To reduce the HSFR, some methods are proposed. Mechanical polishing[48] is the simplest smoothing method which is mainly used to remove typical diamond turning structures. As shown in the Figure 16, it reduced HSFR by more than 10 times through the method. Ion beam polishing

https://doi.org/10.1017/hpl.2023.53 Published online by Cambridge University Press

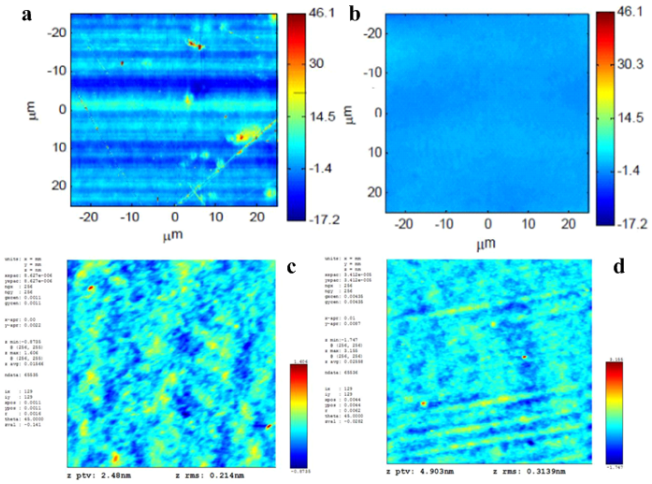

Figure 17. HSFR results (AFM) of adding a smoothing layer by Rigaku: (a) Diamond turned surface sample, (b) Smoothed diamond turned surface sample, (c) 0.14∼0.29nm rms over 2.2um scans and (d) 0.29∼0.39nm rms over 8.7um scans of the grating surface. Figure from Ref. [8, 34]

technology[69,70], which is commonly used on the collectors without gratings, uses the neutral ion beam to bombard the workpiece, removing atoms or molecules in a certain area of the surface, and achieve the ultra-smooth polishing. The method of adding a smoothing layer[71] refers to manufacture a film on the substrate with a smaller HSFR to smooth the roughness, and the performance can be seen in the Figure 17 (a) and (b). Stock et al.[72] used the electron beam evaporation method to deposit a single layer of carbon on the substrate of BK7 and Zerodur to smooth the roughness. Salmassi et al.[73,74] proposed a spin-on-glass resist process based on HSQ to smooth the substrate with diamond-turned structures and presented a roughness reduction from 3.7nm to 0.39nm rms on the Al substrate. Rigaku[8] used a glassy smoothing layer on the substrate grating to reduce HSFR of the surface, achieving the results presented in Figure 17 (c) and (d), which is sufficient for the high performance. Ulmer et al.[75] designed a mirror with a diameter of 1 meter and smoothed the NiP substrate by covering the CNx layer.

4.3.3. Metrology During the preparation of the substrate grating, some measurements are needed to measure the machining accuracy and the overall device performance. The three main aspects to be measured are roughness, reflectivity for different wavelengths and uniformity of reflectivity.

Roughness The thickness of the multilayers deposited on the substrate grating is at the level of nanometer, thus the morphology and roughness of the substrate will be translated to top layers[54,71,76]. It's clear that the prerequisite for reducing the roughness of the multilayers is to reduce the roughness of the substrate grating. The evaluation indicators for roughness include the average roughness, root mean square (RMS) roughness, peak to valley (PV) value, power spectral density (PSD), etc. The first three are simple statistical parameters and only the vertical component of surface roughness is calculated[71]. The PSD measures the roughness from the perspective of Fourier spectral, thereby obtaining the spatial frequency distribution of the surface error, which means it also contains the transverse and longitudinal information of the surface[77,78].

Roughness in different spatial frequency range should be measured by different methods, as shown in Figure 18. According to the scattering theory, the scattering caused by roughness in different spatial frequencies can be generally divided into the following three types[76,79–81]:

(1) Minimum angle scattering caused by low spatial frequency roughness (LSFR), which introduces basic aberration into the system, will blur the image and reduces the resolution of the optical system.
(2) Small-angle scattering caused by medium frequency roughness (MSFR), also known as the stray light, will reduce the contrast of spatial imaging.
(3) Large-angle scattering caused by HSFR will reduce the light flux reaching the image plane, thus reducing the energy transmission efficiency of the optical system.

Taking Rigaku's work as a reference[8], different spatial frequencies of roughness, corresponding to the above influences, are defined as: LSFR: ≥1mm; MSFR: 1 mm∼10um; HSFR: ≤10um.

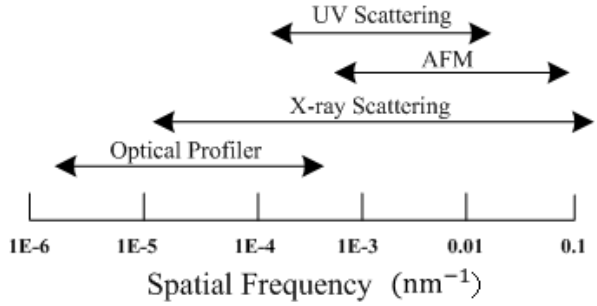

Figure 18. Different measurements for roughness in different spatial frequency. Figure reformed from Ref. [71]

HSFR is a critical indicator to be measured because among the roughness in all frequency bands, the roughness with the spatial wavelength equivalent to the incident light wavelength has the strongest scattering ability[71]. The HSFR of the grating surface used for collector are needed to be less than 0.3nm rms[48,61], which is also the main challenge of the fabrication. At present, the main and most direct method used in HSFR for measuring surfaces with ≤0.1nm rms is Atomic Force Microscope (AFM) measurement, which determines the distance between the probe and the detection surface by the contact force. Its detection area is usually less than tens of microns, the longitudinal resolution is ∼0.01nm[78], and the transverse resolution can generally up

https://doi.org/10.1017/hpl.2023.53 Published online by Cambridge University Press

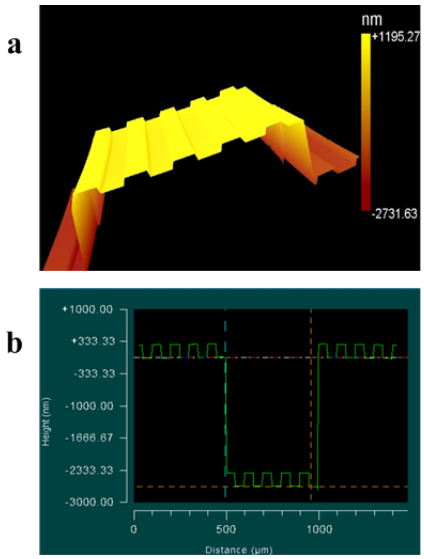

Figure 19. WLI analysis of dual-layer rectangular substrate grating structure by IOF. Figure from Ref. [61, 68]

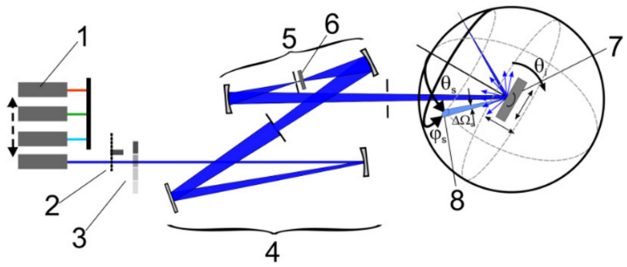

Figure 20. ARS instrument ALBATROSS for scattering measurements in the UV-VIS-IR range. Components: laser sources (1), mechanical chopper for lock-in amplification (2), attenuation filters (3), beam preparation optics (4) with spatial filter (5), polarizer (6), sample (7), and detector (8). For. Figure from Ref. [48]

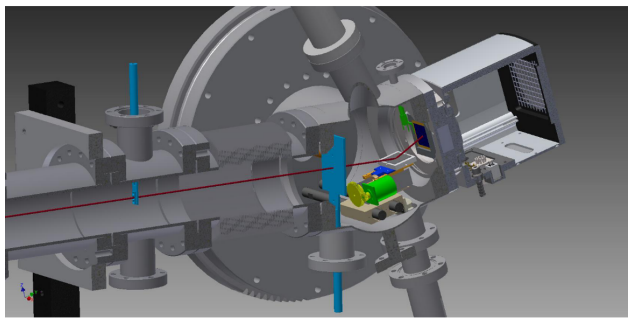

Figure 21. EUV-ARS for the characterization of nanometre structures exposed by PTB. Figure from Ref. [87]

to 0.1nm[71,77], which depends on the radius of curvature of the probe and the depth from the top of the probe to the detection surface[71,82]. In the IOF's experiments on the dual-layer rectangular grating[36,68], with a scanning range of 10um × 10um, the roughness of four facets of the grating were all below 0.25nm rms. It should be noted that if PSD is used for characterization, it is necessary to measure the same surface at different locations and meet the sampling theorem.

LSFR is primarily measured by optical profilometry, including the white light interferometry (WLI), double-beam interferometry, etc., and among which WLI is the main method currently used. WLI is a non-contact metrology, and has the advantages of large measuring range, high vertical accuracy, and fast measuring speed. Based on the principle of optical interference, WLI can analyze the relative height variation of the sample surface according to the contrast and position of the light interference fringe, thus generating a 3D image, and obtaining the 3D morphology and surface roughness of the measured sample. However, due to the influence of dispersion, its lateral accuracy can only reach the scale of hundreds of nanometers[77,78]. IOF[36] used the WLI to characterize the profile of its dual-layer substrate grating, as Figure 19 shows, and controlled the maximum error of the grating period, fill factor and groove depth within less than 1%. Rigaku[8] also used an interference microscope to measure the roughness of the substrate grating, and achieved a LSFR of 0.577um rms.

MSFR can be measured by the laser speckle interferometry and light scattering measurement, both of which are indirect measurement. The former is primarily used in the detection range where the roughness is greater than the illumination wavelength[71], and has the advantages of simple operation and a large measurement range. The brightness, shape and contrast of the speckles generated by the coherent wave can effectively reflect the distribution of surface roughness. Light scattering measurement mainly includes the angle resolved scattering (ARS) measurement and total integrated scattering (TIS) measurement[83]. ARS determines the roughness according to the distribution of the scattered light intensity in the plane[84], while TIS determines the roughness according to the ratio of the light intensity in the hemisphere to the light intensity reflected on the surface of the sample[85]. Compared with TIS, ARS is more complex and expensive, but it can correctly measure the spatial distribution of scattered light and obtain more roughness information[83]. Trost et al.[48] used the ALBATROSS (Figure 20), developed by IOF, to measure the roughness of the multilayer grating. Hilpert et al.[86] measured the roughness of the reflector in the spaceborne optical system by ARS and obtained a roughness value of 0.1nm rms. Herrero et al. of Physikalisch-Technische Bundesanstalt (PTB)[87] exposed a new tool (EUV-ARS) based on the grazing incidence small-angle X-ray scattering instrument (Figure 21), which allows to study the structural surface by analyzing the scattered light and fluorescence signals, and to achieve the roughness measurement at the nanoscale.

https://doi.org/10.1017/hpl.2023.53 Published online by Cambridge University Press

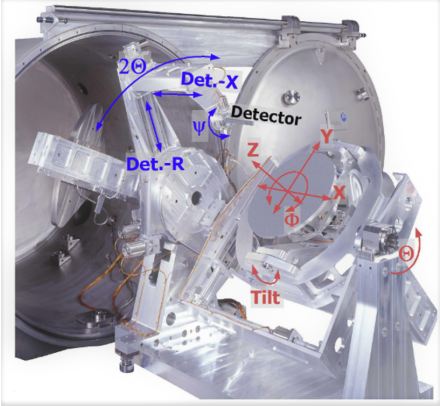

Figure 22. Mechanics of the EUV-reflectometer by PTB. Figure from Ref. [92]

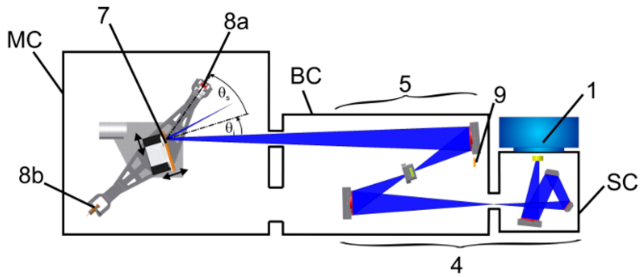

Figure 23. EUV (13.5nm) measurement instrument MERLIN by IOF. Components: the measurement vacuum chamber (MC), beam preparation vacuum chamber (BC), source vacuum chamber (SC), Xe-plasma (1) beam preparation optics (4), spatial filter (5), sample (7), detectors (8a photo diode, 8b - channeltron), and reference detector (9). Figure from Ref. [48]

OoB suppression and EUV Reflectivity The collector integrated with rectangular gratings is designed to suppress 10.6um and 1064nm IR without reducing EUV, so it is necessary to detect the intensity of EUV and IR at the focal plane. Compared with the collector without the grating structure, the intensity of IR at IF generally needs to be suppressed for more than 99%[12], while the minimum loss of EUV achieved nowadays is ∼4.81%[88].

For the EUV detection, the equipments used include the EUV reflectometry at BESSY II developed by PTB in Germany[89–92] (Figure 22), the EUV Reflectometry by National Institute of Standards and Technology (NIST) in the United States[93], and the system MERLIN of IOF[94] (Figure 23).

For the detection of IR suppression, ALBATROSS[95] can also be used. In fact, ALBATROSS is a device that can measure the reflected light, transmitted light and scattered light distribution with high dynamic range, high sensitivity, low noise. What's more, the measurement device can also be custom-built for the actual measuring needs, as shown in the Figure 24. The laser firstly passes through the beam expander, chopper, etc., and is then reflected by the virtual light source sphere before being incident on the full-size collector. After being deflected by a folded plane mirror, it is focused on the HgCdTe detector for the measurement.[8]

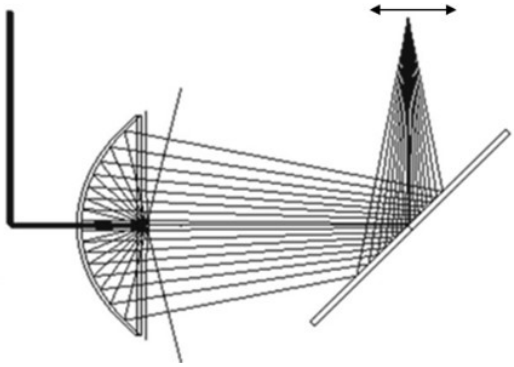

Figure 24. Schematic of the IR Suppression Test Stand. Figure from Ref. [8]

Reflectivity uniformity The final step in the preparation of substrate grating is to deposit Mo /Si multilayers, which aims to improve the EUV reflection performance, so measuring the EUV reflectivity uniformity is very important. Using the EUV reflectometry mentioned above to symmetrically select multiple positions on the collector's surface along the x and y axes, and measure their reflectivity for comparison. IOF[36] used the system of PTB to compare the average EUV reflectivity of the collector integrated with the dual-layer grating, and the change of EUV reflectivity is ∼0.5%. Rigaku[8] used the same system as IOF to measure the peak EUV reflectivity of the collector surface, and showed a variation of less than 0.0025nm at the opposite positions, referring to 0.02% PV variation.

4.3.4. Grating with other shapes According to the existing technical schemes, the collector substrate of the rectangular grating structure cannot effectively filter the DUV, so it is proposed to use the blazed grating to replace the rectangular grating since the structure was theoretically demonstrated effective at filtering out the full-OoB radiations by Boogaard et al.[15] when studying the multilayer grating.

Johnson[67,97] designed a collector integrated with the blazed grating structure which aims to divert the EUV into the IF rather than diffracting IR out of IF, as shown in Figure 25 (a), and two fabrication methods are given which are the conformal-multilayer grating and patterned-multilayer grating. What's more, a power recyling component was designed surrounding the IF aperture to retroreflect IR for a higher source conversion efficiency (CE). Followed that, Hassanein et al.[96] continued the design of the blazed grating and furthered the idea of power recycling, which showed a potential 60% gain of EUV-CE with the preliminary plasma simulation, as shown in Figure 25 (b). However, these relevant researches based on the substrate blazed grating are mainly theoretical analyses, but no experiments have been

https://doi.org/10.1017/hpl.2023.53 Published online by Cambridge University Press

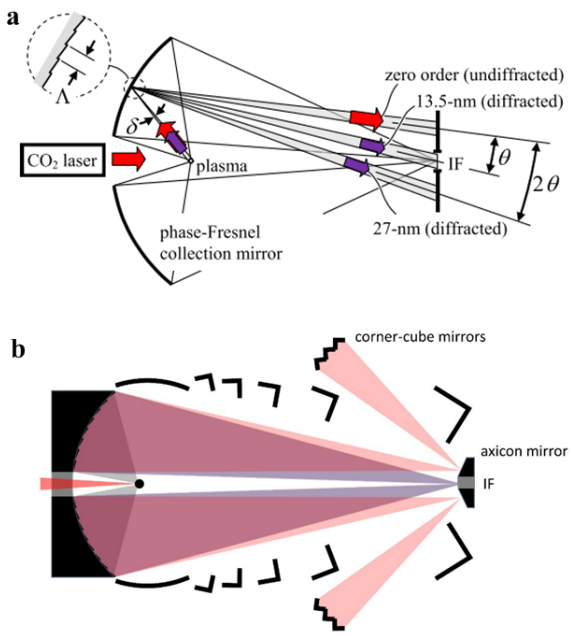

Figure 25. (a) Schematic of the collector integrated with the blazed substrate grating, (b) Schematic of the collector with power recycling mirrors. Figure from Ref. [67, 96]

carried out to figure out the feasibility of this scheme.

Theoretically, the blazed grating can indeed suppress the radiation of IR and UV bands, but the problem lies in the limitations of the manufacturing process. For example, it is difficult to control the blazed angle of the multilayers within 3° [35]. Therefore, its actual effect is far from reaching the theoretical effect, so it is still at the theoretical stage.

5. Conclusions and Expectations

As the most precise manufacturing process in the world today, lithography technology imposes very high requirements for the purity of its high power EUV light source. For the LPP-EUVL system, the OoB with the greatest impact is IR(i.e., 1064nm and 10.6um) and DUV, the former of which causes thermal effect and reduces the pattern accuracy, while the latter one leads to CD errors. Therefore, the intensity of IR needs to be less than 10% and DUV needs to be only 1% of that of EUV at the wafer to avoid the potential damages, while the intensity of EUV must be as high as possible.

Taking the above conditions as the basic indicators for evaluating the SPF for EUVL, it can be found that the traditional free-standing SPFs can barely satisfy the suppression requirements of IR and DUV, and also lead to an EUV loss of $\sim$30% [88]. However, some new free-standing filters have been proposed in recent years and have shown a good performance, such as the DGLm by ASML which suppressed 99% of DUV and 80% of IR while the EUV transmittance reached 85%. Though it may have problems of non-ideal mechanical strength and an extra optical element, it still shows the potential as an SPF for EUVL, especially for the suppression of DUV, as it produces less thermal damage to the optical elements, compared to the IR.

The scheme of taking the micro-structures, integrated onto the collector, as the SPF for EUVL light source also seems to be feasible and effective, especially the substrate grating structure which avoids the process difficulty of stacking thousands of layers. According to the achievements of current researches, Gigaphoton has already obtain an IR suppression of 0.37% at IF while the reduction of EUV reflectivity with unpolarized incident laser is only around 4% compared with the non-structured collector, which represents a better performance than free-standing SPFs. Besides that, this scheme allows a superior mechanical strength, and some designs can be applied onto the collector to relieve the thermal effect, such as the water-cooled device.

The existed designs of the collector integrated with the substrate grating still need to be optimized. For the rectangular grating which has been studied maturely, it only suppresses finite and specific wavelengths, and there's no research shows its suppression capacity in DUV band so far. Therefore, how to suppress IR at the same time of DUV is the problem remained. There's probably three ways to go. One is to adopt the scheme of integrating the collector with the blazed substrate grating. This method raises difficulties of stacking lots of layers which has been the challenge for years, and also, manufacturing the periodic blazed grating on such a large collector is not easy. One is to further develop the membrane which is manageable to suppress all OoBs, just like DGLm, but this faces the problem of being broken easily by the thermal effect from CO_2 laser and will increase the cost of maintenance. Another is to combine two schemes, which means integrating the collector with rectangular gratings, meanwhile, use a transmissive SPF membrane. The similar method has been explored by Suzuki et al.[19], but they use two free-standing SPFs (one for IR, one for DUV) which obviously represents a less mechanical strength than the collector. Thus, there's still room for the improvement of the spectral purity of the EUV light source.

Besides the designs of SPFs for EUVL light source, the metrology also needs to be improved. As the development of the semi-industry, the metrologies that can deal with the smaller and more complex nano-structures are needed. There's no doubt that the scattering metrology plays an important role in this field. To achieve a higher sensitivity, the grazing incidence small angle X-ray scattering is often used, but it has the problem of large footprints of the beam, which needed to be resolved in a more general solution. Using a larger incident wavelength as the source which allows a larger incident angle, may relieve this problem without reducing the sensitivity. Herreroa's work[87] gives some suggestions in this aspect. Another problem that limits the performance of the measuring is the speed of the measurement, in particular, when measuring the surface

https://doi.org/10.1017/hpl.2023.53 Published online by Cambridge University Press

roughness, the ARS needs a lot of time to detect the scattering distribution in the hemisphere space, which can be relieved by the improvement of the scattering model to some extent, such as the regional scattering model by Wang et al.[98] Efforts shall be made on the designs of measuring devices as well as the metrologies in order to meet the requirements of measuring nano-structures.

This paper reviews the development of the SPFs for EUVL, and investigates the key technologies of filtering out OoB radiations for EUVL. The main challenges and developing trends are also discussed in the view of practical applications for the further improvement. It can be seen that the design and manufacture of SPFs for EUVL is not a single task, it requires a coordinated advancement in design methods, process manufacturing and metrologies.

Acknowledgement

This work was supported by Science and Technology Commission of Shanghai Municipality (No.22DZ1100300).

References

1. G. E. Moore, "The future of integrated electronics", https://www.computerhistory.org/collections/catalog/102770836 (August 19, 1965).
2. J. W. S. Rayleigh, *The theory of sound* (Dover Publications, New York, 1945).
3. N. Zong, W. M. Hu, Z. M. Wang, X. J. Wang, S. J. Zhang, Y. BO, Q. J. Peng, Z. Y. XU, "Research progress on laser-produced plasma light source for 13.5 nm extreme ultraviolet lithography" (in Chinese), Chin. Opt. 13, 28 (2020).
4. T. Tomie, "Tin laser-produced plasma as the light source for extreme ultraviolet lithography high-volume manufacturing: history, ideal plasma, present status, and prospects", J. Micro-Nanolith. MEM. 11, 021109 (2012).
5. Y. Teramoto, B. Santos, G. Mertens, R. Kops, M. Kops, A. van Wezyk, H. Yabuta, A. Nagano, T. Shirai, N. Ashizawa, K. Nakamura, K. Kasama, "High-radiance LDP source for mask-inspection application", in *Extreme Ultraviolet (EUV) Lithography VI*, O. R. Wood II, E. M. Panning, ed. (Academic, San Jose, CA, USA, 2015), p. 94220F.
6. N. Lin, W. H. Yang, Y. Y. Chen, X. Wei, C. Wang, J. L. Zhao, Y. J. Peng; Y. X. Leng, "Research Progress and Development Trend of Extreme Ultraviolet Lithography Source" (in Chinese), Laser Optoelectron. P. 59, 0922002 (2022).
7. I. Fomenkov, A. Schafgans, D. Brandt, "Laser-Produced Plasma Sources for High-Volume-Manufacturing EUV Lithography", Synchrotron Radiat. News 32, 3 (2019).
8. M. Kriese, Y. Platonova, B. Ehlersa, L. Jianga, J. Rodrigueza, U. Muellerb, J. Danielb, S. Khatrib, A. Magruderb, S. Granthamc, C. Tarrioc, and T. Lucatortoc, "Development of an EUVL collector with infrared radiation suppression", in *Extreme Ultraviolet (EUV) Lithography V*, O. R. Wood II, E. M. Panning, ed. (Academic, San Jose, CA, USA, 2014), p. 90483C.
9. B. Rollinger, "Droplet target for laser-produced plasma light sources", PhD. Thesis (ETH Zurich, 2010).
10. V. Bakshi, *EUV lithography* (SPIE Press, Bellingham WA, 2018).
11. D. K. Yang, D. Wang, Q. Huang, Y. Song, J. Wu, W. Li, Z.-S. Wang, X. Tang, H. Xu, S. Liu, and C. Gui, "The development of laser-produced plasma EUV light source", Chip. 1, 100019 (2022).
12. V. Bakshi, *EUV Sources for Lithography* (SPIE Press, Bellingham WA, 2006).
13. C. Wagner, N. Harned, "Lithography gets extreme", Nat. Photonics 4, 24 (2010).
14. F. Liu, F. van de W. M. Bayraktar, F. Bijkerk, D. Smeets, S. Huang, Y. Ni, A. Yakunin, P. Havermans, R. Oesterholt, F. Torretti, J. Scheers, and O. Versolato, "Lithography machine in-line broadband spectral metrology", https://www.euvlitho.com/2019/P43.pdf (June, 2019).
15. A.J.R. van den Boogaard, E. Louis, F. A. van Goor and F. Bijkerk, "Optical element for full spectral purity from IR-generated EUV light sources", in *Alternative Lithographic Technologies*, F. M. Schellenberg, B. M. L. Fontaine, ed. (Academic, San Jose, CA, USA, 2009), p. 72713B.
16. M. van de Kerkhof, F. Liu, M. Meeuwissen, X. Zhang, R. de Kruif, N. Davydova, G. Schiffelers, F. Waelisch, E. van Setten, W. Varenkamp, K. Ricken, L. de Winter, J. McNamara, M. Bayraktar, N. M. Felix, and A. Lio, "Spectral purity performance of high- power EUV systems", in *Extreme Ultraviolet (EUV) Lithography XI. SPIE*, N. M. Felix, A. Lio, ed. (Academic, San Jose, CA, USA, 2020), p. 1132321.
17. M. van de Kerkhof, F. Liu, M. Meeuwissen, X. Zhang, M. Bayraktar, R. de Kruif, and N. Davydova, "High-power EUV lithography: spectral purity and imaging performance", J. Micro-Nanolith. MEM. 19,033801(2020).
18. M. Bayraktar, F. A. van Goor, K. J. Boller, and F. Bijkerk, "Spectral purification and infrared light recycling in extreme ultraviolet lithography sources", Opt. Express 22, 8633 (2014).
19. Y. Suzuki, K. Totsu, M. Moriyama, M. Esashi, and S. Tanaka, "Free-standing subwavelength grid infrared cut filter of 90 mm diameter for LPP EUV light source Yukio", Sensor Actual A-Phys. 231, 59 (2015).
20. C. M. Park, I. Kim, S. H. Kim, D. W. Kim, M. S. Hwang, S. N. Kang, C. H. Park, H. W. Kim, J. H. Yeo, and S. S. Kim, "Prospects of DUV OoB suppression techniques in EUV lithography", in *Extreme Ultraviolet (EUV) Lithography V*, O. R. Wood II, E. M. Panning, ed.

https://doi.org/10.1017/hpl.2023.53 Published online by Cambridge University Press

(Academic, San Jose, CA, USA, 2014), p. 90480S.

21. W. A. Soer, M. J. J. Jak, A. M. Yakunin, M. M. J. W. Herpen, and V. Y. Banine, "Grid spectral purity filters for suppression of infrared radiation in laser-produced plasma EUV sources", in *Alternative Lithographic Technologies*, F. M. Schellenberg, B. M. L. Fontaine, ed. (Academic, San Jose, CA, USA, 2009), p. 72712Y.
22. S. A. George, P. P. Naulleau, S. Rekawa, E. Gullikson, and C. D. Kemp, "Out-of-Band Exposure Characterization with the SEMATECH Berkeley 0.3-NA Microfield Exposure Tool", in *Alternative Lithographic Technologies*, F. M. Schellenberg, B. M. L. Fontaine, ed. (Academic, San Jose, CA, USA, 2009), p. 72710X.
23. G. F. Lorusso, N. Davydova, M. Eurlings, C. Kaya, Y. Peng, K. Feenstra, T. H. Fedynyshyn, O. Natt, P. Huber, C. Zaczek, S. Young, P. Graeupner, and E. Hendrickx, "Deep Ultraviolet Out-of-Band Contribution in Extreme Ultraviolet Lithography: Predictions and Experiments", in *Extreme Ultraviolet (EUV) Lithography II*, B. M. L. Fontaine, P. P. Naulleau, ed. (Academic, San Jose, CA, USA, 2011), p. 79692O.
24. G. Salmaso, R. Maas, "A new generation EUV pellicle to enable future EUV lithographic nodes at enhanced productivity", in *International Conference on Extreme Ultraviolet Lithography 2021*. (Academic, Online Only, 2021), p. 118540R.
25. O. Romanets, K. Ricken, M. Kupers, F. Wahlisch, C. Piliego, P. Proman, D. de Graaf, U. F. Behringer, and J. Finders, "Progress in imaging performance with EUV pellicles", in *35th European Mask and Lithography Conference*, U. F.W. Behringer, J. Finders, ed. (Academic, Dresden, Germany, 2019), p.111770Z.
26. M. S. Bibishkin, N. I. Chkhalo, S. A. Gusev, E. B. Kluenkov, A. Y. Lopatin, V. I. Luchin, A. E. Pestov, N. N. Salashchenko, L. A. Shmaenok, N. N. Tsybin, and S. Y. Zuev, "Multilayer Zr/Si filters for EUV lithography and for radiation source metrology", in *Micro- and Nanoelectronics 2007*, K. A. Valiev, A. A. Orlikovsky, ed. (Academic, Zvenigorod, Russian Federation, 2007), p. 702502.
27. N. I. Chkhalo, A. A. Orlikovsky, M. N. Drozdov, E. B. Kluenkov, A. Y. Lopatin, V. I. Luchin, A. E. Pestov, N. N. Salashchenko, L. A. Shmaenok, and N. N. Tsybin, "Influence of annealing on the structural and optical properties of thin multilayer EUV filters containing Zr, Mo and silicides of these metals", in *nternational Conference on Micro- and Nano-Electronics 2009*, K. A. Valiev, A. A. Orlikovsky, ed. (Academic, Zvenigorod, Russian Federation, 2009), p. 752105.
28. S.S. Andreev, E.B. Kluenkov, A.Ya. Lopatin, V.I. Luchin, K.A. Prokhorov, N.N. Salashchenko, L.A. Suslov, and S. Y. Zuev, "Filters for the range of extreme ultraviolet radiation based on myltilayers Zr/Si, Nb/Si, Mo/Si and Mo/C" (in Russian), Poverhnost N2, 6 (2003) .
29. N. I. Chkhalo, M. N. Drozdov, E. B. Kluenkov, A. Y. Lopatin, V. I. Luchin, N. N. Salashchenko, N. N. Tsybin, L. A. Sjmaenok, V. E. Banine, and A. M. Yakunin, "Free-standing spectral purity filters for extreme ultraviolet lithography", J. Micro-Nanolith. MEM. 11, 021115 (2012).
30. M. van de Kerkhof, H. Jasper, L. Levasier, R. Peeters, R. van Es, J.-W. Bosker, A. Zdravkov, E. Lenderink, F. Evangelista, P. Broman, B. Bilski, and T. Last, "Enabling sub-10nm node lithography: presenting the NXE:3400B EUV scanner", in *Extreme Ultraviolet (EUV) Lithography VIII*, E. M. Panning, K. A. Goldberg, ed. (Academic, San Jose, CA, USA, 2017), p. 101430D.
31. G. Rispens and R. Maas, "Removing all EUV resist outgassing requirements", http://ieuvi.org/TWG/Resist/2016/20161023/01_fan_agenda.pdf (October 23, 2016)
32. R. v. Es, M. v. d. Kerkhof, A. Minnaert, G. Fisser, J. d. Klerk, J. Smits, R. Moors, E. Verhoeven, L. Levasier, R. Peeters, M. Pieters, H. Meiling, "EUV for HVM: towards an industrialized scanner for HVM NXE3400B performance update", in *Extreme Ultraviolet (EUV) Lithography IX*, K.h A. Goldberg, ed. (Academic, San Jose, CA, USA, 2018), p. 105830H.
33. H. Kierey, K. Heidemann, B. Kleemann, R. Winters, W. E. W. Singer, F. Melzer, R. Wevers, and M. Antoni, "EUV spectral purity filter: optical and mechanical design, gratings fabrication, and testing Holger", in *Advances in Mirror Technology for X-Ray, EUV Lithography, Laser, and Other Applications*, A. M. Khounsary, U. Dinger, K. Ota, ed. (Academic, Bellingham, WA, USA, 2004), p. 70.
34. Y. Platonov, M, Kriese, R. Crucet, Y. Li, V. Martynov, L. Jiang, J. Rodriguez, U. Mueller, J. Daniel, S. Khatri, A.m Magruder, S. Grantham, C. Tarrio, T. B. Lucatorto, "Collector development with IR suppression and EUVL optics refurbishment at RIT", https://www.euvlitho.com/2013/S30.pdf (November 3, 2013)
35. L.C. Zhang, "Multilayer Grating Technologies for EUV" (in Chinese), OME Information 28, 5 (2011).
36. T. Feigl, M. Perske, H. Pauer, T. Fiedler, U. Zeitner, R. Leitel, H.-C. Eckstein, P. Schleicher, S. Schrder, M. Trost, S. Risse, R. Steinkopf, F. Scholze, and C. Laubis, "Sub-aperture EUV collector with dual-wavelength spectral purity filter", in *Extreme Ultraviolet (EUV) Lithography VI*, O. R. Wood, E. M. Panning, ed. (Academic, San Jose, CA, USA 2015), p. 94220E.
37. H. Nakarai, T. Abe, H. Tanaka, Y. Watanabe, T. Hori, T. Kodama, Y. Shiraishi, T. Yanagida, G. Soumagne, T. Yamada, and T. Saitou, "EUV/DUV source

https://doi.org/10.1017/hpl.2023.53 Published online by Cambridge University Press

development and its collaboration with Germany", https://www.fraunhofer.jp/content/dam/japan/ja/documents/Events/2019/Fraunhofer_Symposium_Oct19/Presentations/%E2%91%A2FHI-Digital%20photonics-2019-GPI-11%20(004).pdf (2019)

38. M. Moriya, O. Wakabayashi, and G. Soumagne, "Mirror for extreme ultra violet, manufacturing method for mirror for extreme ultra violet, and far ultraviolet light source device," U. S. patent 8,592,787,B2 (November, 26, 2013).
39. A.J.R. van den Boogaard, F.A. van Goor, E. Louis, and F. Bijkerk, "Wavelength separation from extreme ultraviolet mirrors using phaseshift reflection", Opt. Lett. 37, 160 (2012).
40. C. Kittel, P. McEuen, *Introduction to solid state physics* (John Wiley & Sons, Singapore, 2018).
41. A. Haase, *Multimethod Metrology of Multilayer Mirrors Using EUV and X-Ray Radiation* (Technische Universitaet, Berlin, 2017).
42. S. Migura, "Optics for EUV Lithography", https://www.euvlitho.com/2019/P24.pdf (June, 2019).
43. K. L. Guen, J. M. Andr, M. Wu, V. Ilakovac, F. Delmotte, S. de Rossi, F. Bridou, E. Meltchakov, A. Giglia, S. Nannarone, "Kossel effect in periodic multilayers", J. Nanosci. Nanotechno. 19, 593 (2019).
44. H. G. J. Moseley, The London, "The high-frequency spectra of the elements", Edinburgh and Dublin Philosophical Magazine and Journal of Science 26, 1024 (1913).
45. V. V. Medvedev, A. J. van den Boogaard, R. van der Meer, A. E. Yakshin, E. Louis, V. M. Krivtsun, and F. Bijkerk, "Infrared diffractive filtering for extreme ultraviolet multilayer Bragg reflectors", Opt. Express 21, 16964 (2013).
46. D. M. Miles, J. A. McCoy, R. L. McEntaffer, C. M. Eichfeld, G. Lavallee, M. Labella, W. Drawl, B. Liu, C. T. DeRoo, and T. Steiner, "Fabrication and Diffraction Efficiency of a Large-format, Replicated X-Ray Reflection Grating", Astrophys. J. 869, 95 (2018).
47. Q. Huang, M. de Boer, J. Barreaux, D. M. Paardekooper, T. van den Boogaard, R. van de Kruijs, E. Zoethout, E. Louis, and F. Bijkerk, "Spectral purity enhancement for the EUV lithography systems by suppressing UV reflection from multilayers", in *Extreme Ultraviolet (EUV) Lithography VE*, O. R. Wood, E. M. Panning, ed. (Academic, San Jose, CA, USA, 2014), p. 90480G.
48. M. Trost, S. Schroder, A. Duparre, S. Risse, T. Feigl, U. D. Zeitner, and A. Tunnermann, "Structured Mo/Si multilayers for IR-suppression in laser-produced EUV light sources", Opt. Express 21, 27852 (2013).
49. E. Spiller, "Evaporated multilayer dispersion elements for soft xrays", in *AIP conference Proceedings*. (Academic, Monterey, CA, USA, 1981), p. 124.
50. E. Spiller, "Reflective multilayer coatings for the far UV region", Appl. Opt. 15, 2333 (1976)
51. P. P. Naulleau,J. A. Liddle, F. Salmassi, E. H. Anderson, E. M. Gullikson, "Design and fabrication of advanced EUV diffractive elements", in *Micromachining Technology for Micro-Optics and Nano-Optics II*, E. G. Johnson, G. P. Nordin, ed. (Academic, San Jose, CA, USA, 2003), p. 9-17.
52. Q. Huang, V. Medvedev, R. van de Kruijs, A. Yakshin, E. Louis, and F. Bijkerk, "Spectral tailoring of nanoscale EUV and soft x-ray multilayer optics", Appl. Phys. Rev. 4, 011104 (2017).
53. P. P. Naulleaua, W. C. Sweattb, and D. A. Tichenorc, "Theoretical efficiency analysis of a condenser-embedded grating-based spectral purity filter for EUV lithography", Opt. Commun. 214, 31 (2002).
54. P. P. Naulleau, J. A. Liddle, E. H. Anderson, E. M. Gullikson, P. Mirkarimi, F. Salmassi, and E. Spiller, "Fabrication of high-efficiency multilayer-coated gratings for the EUV regime using e-beam patterned substrates", Opt. Commun. 229, 109 (2004).
55. P. P. Naulleau, E. H. Anderson, E. M. Gullikson, and J. Bokor, "Fabrication of high-efficiency multilayer-coated binary blazed gratings in the EUV regime", Opt. Commun. 200, 27 (2001).
56. J. A. Liddle, F. Salmassi, P. P. Naulleau, and E. M. Gullikson, "Nanoscale topography control for the fabrication of advanced diffractive optics", J. Vac. Sci. Technol. B 21, 2980 (2003).
57. D. L. Voronov, E. H. Anderson, E. M. Gullikson, F. Salmassi, T. Warwick, V. V. Yashchuk, and H. A. Padmore, "Ultra-high efficiency multilayer blazed gratings through deposition kinetic control", Opt. Lett. 37, 1628 (2012).
58. D. L. Voronov, E. M. Gullikson, F. Salmassi, T. Warwick, and H. A. Padmore, "Enhancement of diffraction efficiency via higher-order operation of a multilayer blazed grating", Opt. Lett. 39, 3157 (2014).
59. Q. Huang, D. M. Paardekooper, E. Zoethout, V. V. Medvedev, R. van de Kruijs, J. Bosgra, E. Louis, and F. Bijkerk, UV spectral filtering by surface structured multilayer mirrors, Opt. Lett. 39, 1185 (2014).
60. Q. Huang, M. de Boer, J. Barreaux, R. van der Meer, E. Louis, and F. Bijkerk, "High efficiency structured EUV multilayer mirror for spectral filtering of long wavelengths", Opt. Express 22, 19365 (2014).
61. T. Feigl, M. Perske, H. Pauer, T. Fiedler, U. Zeitner, R. Leitel, H.-C. Eckstein, P. Schleicher, S. Schrder, M. Trost, S. Risse, R. Steinkopf, C. Laubis, and F. Scholze, "Multilayer EUV optics with integrated IR suppression gratings", https://www.euvlitho.com/2016/P69.pdf (June 15, 2016)
62. H. Mizoguchi, "One Hundred Watt Operation Demonstration of HVM LPP-EUV Source", https://www.euvlitho. com/2014/P2.pdf (June 23, 2014)

https://doi.org/10.1017/hpl.2023.53 Published online by Cambridge University Press

63. H. Mizoguchi, K. M. Nowak, H. Nakarai, T. Abe, T. Ohta, Y. Kawasuji, H. Tanaka, Y. Watanabe, T. Hori, T. Kodama, Y. Shiraishi, T. Yanagida, T. Yamada, T. Yamazaki, S. Okazaki, and T. Saitou, "Update of EUV Source Development Status for HVM Lithography", J. Laser Micro. Nanoeng. 11, 276 (2016).
64. H. Mizoguchi, H. Nakarai, T. Abe, H. Tanak, Y. Watanabe, T. Hori, Y. Shiraishi, T. Yanagida, G. Sumangne, T. Yamada, T. Saitou, N. M. Felix, and A. Lio, "hallenge of¿ 300W high power LPP-EUV source with long mirror lifetime-III for semiconductor HVM", in *Extreme Ultraviolet (EUV) Lithography XII*, N. M. Felix, A. Lio, ed. (Academic, Online Only, 2021), p. 1160919.
65. H. Mizoguchi, H. Nakarai, T. Abe, K. M. Nowak, Y. Kawasuji, H. Tanaka, Y. Watanabe, T. Hori, T. Kodama, Y. Shiraishi, T. Yanagida, G. Soumagne, T. Yamada, T. Yamazaki, S. Okazaki, and T. Saitou, "Performance of 100-W HVM LPP-EUV source", Adv. Opt. Technol. 4, 297 (2015).
66. H. Nakarai, T. Abe, K. M. Nowak, Y. Kawasuji, H. Tanaka, Y. Watanabe, T. Hori, T. Kodama, Y. Shiraishi, T. Yanagida, G. Soumagne, T. Yamada, T. Yamazaki, and T. Saitou, "High-power LPP-EUV source with long collector mirror lifetime for semiconductor high-volume manufacturing", https://www.euvlitho.com/2017/S41.pdf (November 6, 2017),
67. K. C. Johnson, "EUV spectral Purity Filter for Full IR-to-VUV Out-of-Band Rejection, With IR Power Recycling", https://vixra.org/abs/1512.0295 (June 3, 2018)
68. T. Feigl, M. Perske, H. Pauer, and T. Fiedler, "Dual-Wavelength spectral Purity Filter for EUV Collector Mirrors", http://euvlsymposium.lbl.gov/pdf/2014/6056cf3937cc4e17aba94d7bebb27b1e.pdf (October 27, 2014)
69. W. A. Soer, P. Gawlitza, M. M. J. W. v. Herpen, M. J. J. Jak, S. Braun, P. Muys, and V. Y. Banine, "Extreme ultraviolet multilayer mirror with near-zero IR reflectanc", Opt. lett. 34, 3680 (2009).
70. E. Spiller, S. L. Baker, P. B. Mirkarimi, V. Sperry, E. M. Gullikson, and D. G. Stearns, "High-performance Mo-Si multilayer coatings for extreme-ultraviolet lithography by ion-beam deposition", Appl. Opt. 42, 19 (2003).
71. S. M. Zhang, "The Research and Characterization of Cleaning Methods and Smoothing Layer for the Substrate of Extreme Ultraviolet Multilayer " (in Chinese), PhD. Thesis (Tongji Unversity, 2007).
72. H. J. Stock, F. Hamelmann, U. Kleineberg, D. Menke, B. Schmiedeskamp, K. Osterried, K. F. Heidemann, and U. Heinzmann, "Carbon buffer layers for smoothing superpolished glass surfaces as substrates for molybdenum/silicon multilayer soft-x-ray mirrors", Appl. Opt. 7, 1650 (1997).
73. F. Salmassi, P. P. Naulleau, and E. M. Gullikson, "Spin-on-glass coatings for the generation of superpolished substrates for use in the extreme-ultraviolet region", Appl. Opt. 45, 2404 (2006).
74. F. Salmassi, C. N. Anderson, E. M. Gullikson, P. P. Naulleau, "Spin-on-glass smoothing of diamond turned optics for use in the extreme ultraviolet regime", in *Advanced Fabrication Technologies for Micro/Nano Optics and Photonics*, T. J. Suleski, W. V. Schoenfeld, J. J. Wang, ed. (Academic, San Jose, CA, USA, 2008), p. 68830F.
75. M. P. Ulmer, J. H. Dugard, D. Quispe, D. B. Buchholz, S. Stagon, Y.-W. Chung, J. Cao, K. Kritikos, N. Guerra, M. T. Stahl, R. Shiri, R. Vaidyanathan, J.-W. A. den Herder, K. Nakazawa, and S. Nikzad, "A concept for a deployable normal incidence EUV mirror based on shape memory alloy sheets", in *Space Telescopes and Instrumentation 2022: Ultraviolet to Gamma Ray*, J. A. den Herder, S. Nikzad, K. Nakazawa, ed. (Academic, Montral, Qubec, Canada, 2022), p. 1218131.
76. E. Louis, A. E. Yakshin, T. Tsarfati, and F. Bijkerk, "Nanometer interface and materials control for multilayer EUV-optical applications", Prog. Surf. Sci. 86, 255 (2011).
77. J. C. Chen, "Comparison of Ultra-Precision Machined Surface Roughness Measurement Methods and Power spectral Density Characterization" (in Chinese), PhD. Thesis (Harbin Institute of Technology, 2009).
78. L. P, "Surface Topography Evaluation and Error Compensation Based on White Light Interferometry" (in Chinese), Master's Thesis (Dalian University of Technology, 2021).
79. L. Yang, X. L. Zheng, B. Chen, "Calculations of resolution for EUV telescope based on surface roughness of mirrors" (in Chinese), Opt. Precision Eng. 19, 2565 (2011).
80. J. Wang, L. P. Wang, C. S. Jin, Y. Xie, "Analysis method of mirror processing error related to stray light in EUV lithography system" (in Chinese), Chinese patent 104317168 B (March 3, 2016)
81. I. Schuster, W. Merkel, G. Metalidis, and H. Kierey, "EUV Collector", U. S. patent 10,503,075 B2 (Dec 10, 2019).
82. Eastman J, Bausmeister P, "The microstructure of polished optical surfaces", Opt. Commun. 12, 418 (1974).
83. L. Mazule, S. Liukaityte, R. C. Eckardt, A. Melninkaitis, O. Balachninaite and V. Sirutkaitis, "A system for measuring surface roughness by total integrated scattering", J. Phys. D: Appl. Phys. 44, 505103 (2011).
84. J. Bhm, M. Jech, M. Vellekoop, "Analysis of NM-Scale Scratches on High-Gloss Tribological Surfaces by Using an Angle-Resolved Light Scattering Method", Tribol. Lett. 37, 209 (2010).

https://doi.org/10.1017/hpl.2023.53 Published online by Cambridge University Press

85. C. Wei, "Surface Quality Detection Technology of Optical Components Based on Regional Scattering" (in Chinese) , Master's Thesis (Xi'an Technological Unitversity, 2022).
86. E. Hilpert, J. Hartung, H. von Lukowicz, T. Herffurth, N. Heidler, "Design, additive manufacturing, processing, and char- acterization of metal mirror made of aluminum silicon alloy for space applications", Opt. Eng. 58, 092613 (2019).
87. A. F. Herrero, H. Mentzel, V. Soltwisch, S. Jaroslawzew, C. Laubis, and F. Scholze, "EUV-angle resolved scatter (EUV- ARS): a new tool for the characterization of nanometre structures", in *Metrology, Inspection, and Process Control for Microlithography XXXII*, V. A. Ukraintsev, O. Adan, ed. (Academic, San Jose, CA, USA, 2018), p. 105850P.
88. S. Sun, C. Jin, B. Yu, T. Guo, S. Yao, W. Deng, and C. Li, "Modeling multilayer coating profiles with defects on EUV collector with grating", Opt. Eng. 58, 107102 (2019).
89. A. E. Yakshin, I. V. Kozhevnikov, E. Zoethout, E. Louis, and F. Bijkerk, "Properties of broadband depth-graded multilayer mirrors for EUV optical systems", Opt. Express 18, 6957 (2010).
90. C. Laubis, A. Barboutis, M. Biel, C. Buchholz, B. Dubrau, A. Fischer, A. Hesse, C. Stadelhoff, V. Soltwisch and F. Scholze, "Status of EUV Reflectometry at PTB", in *Extreme Ultraviolet (EUV) Lithography IV*, P. P. Naullea, ed. (Academic, San Jose, CA, USA, 2013), p. 867921.
91. C. Laubis, A. Barboutis, C. Buchholz, A. Fischer, A. Haase, F. Knorr, H. Mentzel, J. Puls, A. Schnstedt, M. Sintschuk, V. Soltwisch, C. Stadelhoff, F. Scholze, "Update on EUV radiometry at PTB", in *Proc. of SPIE*, E. M. Panning, K. A. Goldberg, ed. (Academic, San Jose, CA, USA, 2016), p. 977627.
92. F. Scholze, C. Laubis, U. Dersch, J. Pomplun, S. Burgerc, F. Schmidt, "The influence of line edge roughness and CD uniformity on EUV scatterometry for CD characterization of EUV masks", in *Modeling Aspects in Optical Metrology*, H. Bosse, B. Bodermann, R. M. Silver ed. (Academic, Munich, Germany, 2007), p. 66171A.
93. S. Grantham, C. Tarrio,T. Lucatorto, M. Kriese, Y. Platonov, J. Rodriguez, L. Jiang, " Improved measurement capabilities at the NIST EUV reflectometry facility", in *Extreme Ultraviolet (EUV) Lithography V*, O. R. Wood II, E. M. Panni, ed. (Academic, San Jose, CA, USA, 2014), p. 90481.
94. S. Schrder, T. Herffurth, M. Trost, and A. Duparr, "Angle-resolved scattering and reflectance of extreme-ultraviolet multilayer coatings: measurement and analysis", Appl. Opt. 49, 1503 (2010)
95. S. Schrder, T. Herffurth, H. Blaschke, and A. Duparr, "Angle-resolved scattering: an effective method for characterizing thin-film coatings", Appl. Opt. 50, C164 (2011)
96. A. Hassanein, V. Sizyuk, T. Sizyuk, and K. Johnson, "Increasing EUV source efficiency via recycling of radiation power", in *Extreme Ultraviolet (EUV) Lithography IX*, K. A. Goldberg, ed. (Academic, San Jose, CA, USA, 2018), p. 1058319.
97. K. C. Johnson, "Extreme-ultraviolet plasma source with full, infrared to vacuum ultraviolet spectral filtering, and with power recycling Kenneth", J. Vac. Sci. Technol. B 34, 041608 (2016).
98. H. J. Wang, C. Wei, A. L. Tian, B. C. Liu, X. L. Zhu, "Surface roughness detection method of optical elements based on region scattering", in *Tenth International Symposium on Advanced Optical Manufacturing and Testing Technologies*, X. Li, X. M. Duan, M. B. Pu, C. T. Wang, S. Hu, X. G. Lu, ed. (Academic, Chengdu, China, 2021), p. 120730N.

https://doi.org/10.1017/hpl.2023.53 Published online by Cambridge University Press